

# Spin properties of a two dimensional electron system: valley degeneracy and finite thickness effects

R. K. Moudgil,<sup>1,\*</sup> Krishan Kumar,<sup>1,2</sup> and Gaetano Senatore<sup>3,4</sup>

<sup>1</sup>*Department of Physics, Kurukshetra University, Kurukshetra - 136 119, India*

<sup>2</sup>*P.G. Department of Applied Physics, S. D. College, Ambala-Cantt. - 133 001, India*

<sup>3</sup>*Dipartimento di Fisica, Università di Trieste, Strada Costiera 11, 34151 Trieste, Italy*

<sup>4</sup>*CNR-IOM DEMOCRITOS Simulation Center, Trieste, Italy*

(Dated: November 21, 2021)

The spin susceptibility of a two-dimensional electron system is calculated by determining the spin-polarization dependence of the ground-state energy within the self-consistent mean-field theory of Singwi *et al.* (STLS). Results are presented for three different devices, viz. the Si (100) inversion layer, the AlAs quantum well, and the GaAs heterojunction-insulated gate field-effect transistor. We find a fairly good agreement with experiments for the Si (100) system, on most of the experimental density range, whereas the agreement for the AlAs and GaAs systems is less satisfactory; in all cases, however, it is vital to include the characteristic device parameters like the valley degeneracy, the finite transverse thickness, etc. Further, the STLS theory predicts an abrupt spin-polarization transition at a sufficiently low electron density irrespective of the valley degeneracy and/or the finite thickness, with the partially spin-polarized states remaining unstable. Moreover, in the Si (100) inversion layer, the spin-polarization transition is preceded by the simultaneous valley- and spin-polarization; for its zero thickness model, these transitions however grossly disagree with the recent quantum Monte Carlo simulations. This drawback of the STLS theory is traced to its inaccuracy in treating electron correlations, which in turn become more and more important as the number of independent components (spin and valley) increases.

PACS numbers: 71.45.Gm, 71.10.Ca, 73.21.-b, 71.10.-w

## I. INTRODUCTION

Recently, the study of spin properties of a two-dimensional electron system (2DES), realized at the interface of semiconductor-insulator/semiconductor heterojunctions<sup>1</sup>, has attracted a great deal of interest. Envisaged as having its fundamental as well as technological importance (e.g., in spintronics<sup>2</sup>), one of the chief concerns has been to determine the 2D spin phase diagram. In this regard, the recent quantum Monte Carlo (QMC) simulations<sup>3,4</sup> have revealed that the electron correlations may favor a weakly first-order spin-polarization transition at  $r_s \approx 26$  before the evolution of Wigner crystallization at  $r_s \approx 35$ . Unlike in a 3DES<sup>5</sup>, the partially spin-polarized phases were found to be unstable. Here,  $r_s = 1/(a_B \sqrt{n\pi})$ , is the usual coupling parameter with  $n$  as the areal electron density and  $a_B$  the effective Bohr atomic radius. Experimentally, the spin properties have been probed mainly by measuring the spin susceptibility  $\chi_s$ . Quite generally,  $\chi_s$  has been found to grow over its Pauli value  $\chi_P$  with increasing  $r_s$ , the growth depending markedly on the device hosting the 2DES. For the Si (100) inversion layer, Shashkin *et al.*<sup>6,7</sup> and Vitkalov *et al.*<sup>8</sup> have found an indication of a ferromagnetic instability at a density close to the apparent metal-insulator transition (MIT), thus suggesting a relation between the spin-polarization and the MIT. However, Pudalov *et al.*<sup>9</sup> have ruled out the possibility of such an instability for densities down to the MIT, though admittedly in different samples. A qualitatively similar result has been found for 2D electrons in the AlAs/GaAs

based heterostructures<sup>10,11</sup>.

The role of the valley degree of freedom  $g_v$  has also been explored<sup>12</sup> and, contrary to common expectation (based on Hartree-Fock), the spin susceptibility enhancement  $\chi_s/\chi_P$  in the two-valley (2V) state is found to be smaller than the one-valley (1V) result. Note however that, at least at high density the spin susceptibility  $\chi_s$  of the 2V system is indeed larger than the 1V one. Apart from this, the recent QMC simulations of the 2V2DES due to Marchi *et al.*<sup>13</sup> have shown that the spin properties undergo a qualitative change with  $g_v$ . Notably, the 2V2DES did not support the spin-polarization transition, a finding at variance with the 1V QMC result<sup>4</sup>. The discrepancy with the experimental indication of a diverging spin susceptibility found by Shashkin *et al.*<sup>7</sup>, on the contrary, is naturally ascribed to absence of disorder in the QMC simulations. In Ref. 13, an analytical fit to the QMC correlation energy at arbitrary spin polarization  $\zeta$  has also been provided;  $\zeta = (n_\uparrow - n_\downarrow)/(n_\uparrow + n_\downarrow)$ , with  $n_\sigma$  being the density of electrons having spin  $\sigma$ .

Since the measurement of  $\chi_s$ , there have been theoretical attempts<sup>14-16</sup> to elucidate the experimental data. The QMC simulations<sup>4,13</sup> have so far been performed only for an ideal (i.e., zero transverse thickness) 2DES. However, the device-specific parameters such as the transverse thickness of the electron layer, valley degeneracy etc., have been shown<sup>15,16</sup> to have an appreciable effect on  $\chi_s$ . Theoretically, the main problem has consisted in treating the electron correlations, thus making the use of approximations inevitable. Rajagopal *et al.*<sup>17</sup> first determined the spin properties beyond the Hartree-Fock

approximation (HFA) by numerically evaluating the sum of ring diagrams. Zhang and Das Sarma<sup>16</sup> recently used the random-phase approximation (RPA) to deal with the correlations. The correlations were found to introduce quantitative as well as qualitative changes in the ground state. Particularly, the critical  $r_s$  for transition to the ferromagnetic phase increased both for the 1V and 2V states, and the 2V  $\chi_s/\chi_P$  now lays below the 1V result as in simulations<sup>13</sup> and experiment<sup>7</sup>. Davoudi and Tosi<sup>18</sup> went beyond the RPA by including the short-range correlations within the self-consistent mean-field theory of Singwi, Tosi, Land, and Sjölander (STLS)<sup>19</sup>, but they restricted their study to an ideal 1V2DES model. The ferromagnetic instability was found to occur at almost the same  $r_s$  ( $\sim 5.6$ ) as in the RPA. However, the ground-state energy for the partially spin-polarized states could be computed only up to  $r_s \approx 4$  due to the appearance of an unphysical instability and accordingly, the fate of these states was not clear for  $r_s > 4$ . Although no direct comparison with the RPA was drawn, yet it is known that the RPA is accurate only at low  $r_s$ .

A theoretical study of the spin properties of a 2DES by taking into account the correlations and the device details (the transverse thickness and the valley degeneracy) makes the main aim of the present work. The correlations will be treated at the level of STLS approximation. The STLS has been used previously to study these effects<sup>20,21</sup>, but only in the unpolarized phase. Firstly, we intend to examine the ground state for its stability with respect to  $\zeta$  and  $g_v$  by comparing the ground-state energy in different states. Secondly, we shall extract  $\chi_s$  from the  $\zeta$  dependence of ground-state energy. To assess the role of device details,  $\chi_s$  will be calculated for three different experimentally studied devices, namely, the Si (100) inversion layer<sup>7,22</sup>, the AlAs quantum well (QW)<sup>10</sup>, and the GaAs heterojunction-insulated gate field-effect transistor (HIGFET)<sup>11</sup>. For the ideal 2DES model, we shall compare our results with the recent QMC simulations<sup>4,13</sup>. To the best of our knowledge, the STLS theory has not been so far tested against the QMC correlation energy at arbitrary  $\zeta$ .

The rest of the paper is organized as follows: The 2DES model and the STLS formalism are presented in Sec. II. Results and discussion are given in Sec. III. In Sec. IV the paper is concluded with a brief summary.

## II. THEORETICAL FORMALISM

### A. 2DES model

The electrons confined dynamically to a plane, immersed in a rigid charge neutralizing background, with  $e^2/r$  interaction has been the commonly used model to study a 2DES. However, the electrons in actual devices are trapped in a finite QW along the transverse direction, which results in a multi-subband 2DES having a finite transverse thickness. Quite often, it is reasonable

to assume that the electrons occupy only the lowest energy subband. Under these conditions, one has to deal with an effective electron interaction potential<sup>1</sup>

$$V(q) = \frac{2\pi e^2}{\epsilon q} F(q), \quad (1)$$

where  $\epsilon$  is the dielectric constant of the substrate and  $F(q)$  the form factor arising due to the finite thickness of the 2DES. Such a 2D model is often referred to as a quasi 2DES. On setting  $F(q) = 1$ , the ideal 2DES model is recovered. Obviously,  $F(q)$  would depend upon the details of the device hosting the 2DES. For the Si (100) inversion layer, the system of main interest in the present study, we use the model of Stern and Howard<sup>23</sup> where

$$F(q) = \frac{1}{16} \left(1 + \frac{\epsilon_{ins}}{\epsilon_{sc}}\right) \left(1 + \frac{q}{b}\right)^{-3} \left[8 + 9\frac{q}{b} + 3\frac{q^2}{b^2}\right] + \frac{1}{2} \left(1 - \frac{\epsilon_{ins}}{\epsilon_{sc}}\right) \left(1 + \frac{q}{b}\right)^{-6}, \quad (2)$$

and  $\epsilon = (\epsilon_{sc} + \epsilon_{ins})/2$ . Here,  $\epsilon_{sc}$  and  $\epsilon_{ins}$  are, respectively, the dielectric constants of the Si substrate and the insulating SiO<sub>2</sub> layer, and  $b$  is given by

$$b = \left[ \frac{48\pi e^2 m_z}{\epsilon_{sc} \hbar^2} \left( n_d + \frac{11}{32} n \right) \right]^{1/3}, \quad (3)$$

with  $m_z$  being the electron effective mass in the transverse direction and  $n_d$  the electron concentration in the depletion layer. Depending upon the orientation of the Si surface, its conduction band is  $g_v$ -fold degenerate- the so-called valley degeneracy;  $g_v = 2$  for the Si (100) inversion layer. Thus, if  $n_{i\sigma}$  denotes the density of electrons of spin  $\sigma$  in the  $i$ th valley, we must have:  $n = \sum_{i\sigma} n_{i\sigma}$ . Through out our study, we shall take  $T = 0K$ .

### B. Density response function

We use the dielectric approach where the density response of the electron system to an external electric potential  $V^{ext}(q, \omega)$  is a central quantity in determining its ground-state properties. It is assumed<sup>20,21,24</sup> that the inter-valley scattering is negligibly small. The multi-valley electron system can then be treated as a multi-component system, with the valley index  $i$  representing a particular component. At arbitrary  $\zeta$ , the 2V2DES is therefore equivalent to a four-component system and its linear density response function  $\chi_{i\sigma i' \sigma'}(q, \omega)$  is defined as

$$\rho_{i\sigma}^{ind}(q, \omega) = \sum_{i' \sigma'} \chi_{i\sigma i' \sigma'}(q, \omega) V_{i' \sigma'}^{ext}(q, \omega), \quad (4)$$

where  $\rho_{i\sigma}^{ind}(q, \omega)$  represents the induced electron density in the  $i$ th valley for the spin component  $\sigma$ . For the response function calculation, we employ the STLS mean-field approximation, which has earlier been used<sup>18,25</sup> to

study a two-component system. Its extension to the four-component system is straightforward and therefore, only the central relations of the formulation are given here.

The induced density  $\rho_{i\sigma}^{ind}(q, \omega)$  can be compactly expressed as

$$\rho_{i\sigma}^{ind}(q, \omega) = \chi_{i\sigma}^0(q, \omega) [V_{i\sigma}^{ext}(q, \omega) + V_{i\sigma}^{ind}(q, \omega)], \quad (5)$$

where  $\chi_{i\sigma}^0(q, \omega)$  is the density response function of non-interacting electrons having spin  $\sigma$  in the  $i$ th valley and

$$V_{i\sigma}^{ind}(q, \omega) = \sum_{i'\sigma'} \rho_{i'\sigma'}^{ind}(q, \omega) V(q) [1 - G_{i\sigma i'\sigma'}(q)], \quad (6)$$

is the induced potential. Here,  $G_{i\sigma i'\sigma'}(q)$  are the spin- and valley-resolved local-field correction (LFC) factors which account for correlation among electrons in valleys  $i$  and  $i'$  with spins  $\sigma$  and  $\sigma'$ . In the STLS approach,  $G_{i\sigma i'\sigma'}(q)$  are given in terms of the corresponding static density structure factors  $S_{i\sigma i'\sigma'}(q)$  as

$$G_{i\sigma i'\sigma'}(q) = -\frac{1}{\sqrt{n_{i\sigma}n_{i'\sigma'}}} \int \frac{d\mathbf{q}'}{(2\pi)^2} \frac{\mathbf{q} \cdot \mathbf{q}'}{q^2} \frac{V(q')}{V(q)} \times [S_{i\sigma i'\sigma'}(|\mathbf{q} - \mathbf{q}'|) - \delta_{ii'} \delta_{\sigma\sigma'}]. \quad (7)$$

Using Eqs. (4)-(6), the density response matrix  $\chi$  ( $2g_v \times 2g_v$ ) is obtained as

$$\chi = \mathcal{A}^{-1}; \mathcal{A}_{i\sigma i'\sigma'} = \frac{\delta_{ii'} \delta_{\sigma\sigma'}}{\chi_{i\sigma}^0(q, \omega)} - V(q) [1 - G_{i\sigma i'\sigma'}(q)]. \quad (8)$$

The fluctuation-dissipation theorem<sup>26</sup>, which relates  $S_{i\sigma i'\sigma'}(q)$  with  $\chi_{i\sigma i'\sigma'}(q, \omega)$  as

$$S_{i\sigma i'\sigma'}(q) = -\frac{\hbar}{\pi \sqrt{n_{i\sigma}n_{i'\sigma'}}} \int_0^\infty d\omega \chi_{i\sigma i'\sigma'}(q, i\omega), \quad (9)$$

closes the set of STLS equations for the density response matrix. The  $\omega$  integration in Eq. (9) has been performed along the imaginary  $\omega$  axis to avoid the problem of plasmon poles on the real  $\omega$  axis<sup>27</sup>. Evidently, the response function calculation has to be carried out numerically by solving the set of Eqs. (7)-(9) in a self-consistent way.

### C. Ground-state energy and spin susceptibility

The ground-state energy per particle  $E_0$  can be determined by a straightforward extension of the ground-state energy theorem<sup>26</sup> to the multi-component system as

$$E_0 = \frac{1}{n} \sum_{i\sigma} n_{i\sigma} \left( \frac{\hbar^2 k_{F,i\sigma}^2}{4m_b} \right) + \int_0^{\epsilon^2} \frac{d\lambda}{\lambda} E^{int}(\lambda), \quad (10)$$

where the first term is the kinetic energy per electron of the non-interacting system and the second term represents the potential energy contribution. Here,  $m_b$  is

the effective band mass,  $k_{F,i\sigma} = (4\pi n_{i\sigma})^{1/2}$ , is the Fermi wave vector of the valley-spin component  $i\sigma$ , and

$$E^{int}(\lambda) = \frac{1}{2n} \sum_{i\sigma i'\sigma'} E_{i\sigma i'\sigma'}^{int}(\lambda), \quad (11)$$

is the interaction energy per electron with Coulomb coupling  $\lambda$ . Its components  $E_{i\sigma i'\sigma'}^{int}(\lambda)$  are given by

$$E_{i\sigma i'\sigma'}^{int}(\lambda) = \sqrt{n_{i\sigma}n_{i'\sigma'}} \int \frac{d\mathbf{q}}{(2\pi)^2} V(q, \lambda) \times [S_{i\sigma i'\sigma'}(q, \lambda) - \delta_{ii'} \delta_{\sigma\sigma'}]. \quad (12)$$

Thus, the calculation of  $E_0$  is based solely on the set of static structure factors  $S_{i\sigma i'\sigma'}(q, \lambda)$ .

The spin susceptibility  $\chi_s$  can be obtained from the second-order derivative of  $E_0$  with respect to  $\zeta$  as

$$\frac{\chi_s}{\chi_P} = \frac{\pi \hbar^2 n}{g_v m_b} \left[ \left( \frac{\partial^2 E_0}{\partial \zeta^2} \right)_{\zeta=0} \right]^{-1}. \quad (13)$$

Here,  $\chi_P = (g_v m_b g^2 \mu_B^2 / 4\pi \hbar^2)$ , is the Pauli susceptibility, with  $g$  the Lande factor and  $\mu_B$  the Bohr magneton.

The theoretical formalism given above is applicable to an arbitrary  $g_v$  and  $\zeta$ . In the next section, we present numerical results for  $g_v = 2$  and 1.

## III. RESULTS AND DISCUSSION

The numerical calculation proceeds as follows: Eqs. (7)-(9) are solved iteratively for the set of independent partial structure factors  $S_{i\sigma i'\sigma'}(q)$ . These results are then used in Eq. (10) to compute the ground-state energy  $E_0$  and hence, the spin susceptibility  $\chi_s$  from Eq. (13). Except in section III D, the prefix 'quasi' with 2DES refers to the Si (100) inversion layer, where the input parameters used are:  $m_z = 0.98m_e$ ,  $\epsilon_{sc} = 11.8$ ,  $\epsilon_{ins} = 3.8$ , and  $n_d = 1.2 \times 10^{11} \text{cm}^{-2}$ . When two valleys have unequal electron population and partial spin polarization, the calculation of  $E_0$  requires ten independent partial  $S(q)$ 's. However, we restrict here to the symmetric case in which the two valleys have equal population and spin polarization (i.e.,  $n_{1\uparrow} = n_{2\uparrow}$  and  $n_{1\downarrow} = n_{2\downarrow}$ ). With this restriction, the number of independent partial  $S(q)$ 's reduce to five, and the computation of  $E_0$  is greatly simplified as it involves only three independent combinations of  $S_{i\sigma i'\sigma'}(q)$ , viz.  $S_{\uparrow\uparrow}(q) = S_{1\uparrow 1\uparrow}(q) + S_{1\uparrow 2\uparrow}(q)$ ,  $S_{\downarrow\downarrow}(q) = S_{1\downarrow 1\downarrow}(q) + S_{1\downarrow 2\downarrow}(q)$ , and  $S_{\uparrow\downarrow}(q) = 2S_{1\uparrow 1\downarrow}(q)$ . It turns out that  $S_{\uparrow\uparrow}(q)$ ,  $S_{\downarrow\downarrow}(q)$ , and  $S_{\uparrow\downarrow}(q)$  are simply the respective  $S(q)$ 's of a partially polarized electron system with  $g_v$ -fold degenerate  $\uparrow$  and  $\downarrow$  spin states. We begin by discussing  $S_{\sigma\sigma'}(q)$ , as  $E_0$  is solely determined in terms of these. Through out the results presented, the wave vector  $q$  is in units of  $k_{F\uparrow}$  ( $= k_{F,1\uparrow} = k_{F,2\uparrow}$ ), energies in effective Rydberg, and  $\hbar = 1$ .

### A. Spin-resolved static structure factors

We accepted the iterative solution when the convergence in  $S_{\sigma\sigma'}(q)$  was better than  $10^{-6}$ . However, it became almost impossible to obtain the self-consistent solution at and above a critical  $r_s$  (say  $r_s^c$ ); for instance,  $r_s^c \approx 3.1$  at  $\zeta = 0$  for the quasi 2V2DES. We find out that this problem arises due to the emergence of (unphysical) poles in  $\chi_{\sigma\sigma'}(q, \omega)$  on the imaginary  $\omega$  axis over a definite  $q$  interval,  $0 \leq q \leq q_c$ . A qualitatively similar situation was earlier faced for an ideal 1V2DES by Moudgil *et al.*<sup>28</sup> and Davoudi and Tosi<sup>18</sup>, and for a 3DES by two of the present authors<sup>29</sup>. Due entirely to these poles, the authors in Ref. 18 could compute  $E_0$  for the partially spin-polarized states only up to  $r_s \sim 4$ . However, we have shown in Ref. 29 that (i) the self-consistent  $S_{\sigma\sigma'}(q)$  can be obtained for  $r_s$  beyond  $r_s^c$  if the existence of the poles is taken into account in establishing the relation between the frequency integrals of  $\chi''_{\sigma\sigma'}(q, \omega)$  and  $\chi_{\sigma\sigma'}(q, \omega)$ , (ii) although the STLS theory breaks down in describing  $S_{\sigma\sigma'}(q)$  for  $r_s > r_s^c$ , yet it provides a fairly good account of the total charge-charge structure factor  $S_{CC}(q)$ , which in terms of its components is given by

$$S_{CC}(q) = \frac{1+\zeta}{2} S_{\uparrow\uparrow}(q) + \frac{1-\zeta}{2} S_{\downarrow\downarrow}(q) + \sqrt{1-\zeta^2} S_{\uparrow\downarrow}(q). \quad (14)$$

It may be pointed out that the calculation of  $E_0$  relies solely on the knowledge of  $S_{CC}(q)$  [see Eq. (16)]. Taking into account the likelihood of a pole in  $\chi_{\sigma\sigma'}(q, \omega)$  [say at  $\omega = \omega_0(q)$ ], Eq. (9) takes the form<sup>30</sup>

$$S_{\sigma\sigma'}(q) = -\frac{1}{\pi\sqrt{n_\sigma n_{\sigma'}}} \int_0^\infty d\omega \left[ \chi_{\sigma\sigma'}(q, \omega) - \frac{a_{\sigma\sigma'}}{\omega - \omega_0(q)} + \frac{a_{\sigma\sigma'}}{\omega + \omega_0(q)} \right]. \quad (15)$$

Here,  $a_{\sigma\sigma'}$  is related to the first-order residue  $b_{\sigma\sigma'}$  of  $\chi_{\sigma\sigma'}(q, z)$  at  $z = i\omega_0(q)$ , by  $a_{\sigma\sigma'} = -ib_{\sigma\sigma'}$ . Making use of the Eq. (15), we are able to determine the self-consistent  $S_{\sigma\sigma'}(q)$  at any desired  $r_s$  and  $\zeta$  values.

We show in Fig. 1 the self-consistent  $S_{\sigma\sigma'}(q)$  for the quasi 2V2DES at  $\zeta = 0.25$  for  $r_s = 2$  and 4. The sharp peaks at  $r_s = 4$  are the artifact of unphysical poles in  $\chi_{\sigma\sigma'}(q, \omega)$ . In order to elaborate this connection, we have plotted  $\omega_0(q)$  in Fig. 2 at  $\zeta = 0.25$  for two  $r_s$  values. Apparently,  $S_{\sigma\sigma'}(q)$  have peaks precisely at  $q = q_c$  and  $q_c$  increases with  $r_s$ . In fact,  $S_{\sigma\sigma'}(q)$  start exhibiting such peaks for  $r_s$  just above  $r_s^c$  and as  $r_s \rightarrow r_s^c$ , both  $\omega_0(q)$  and  $q_c$  tend to zero. Nevertheless, it is interesting to note that the resulting  $S_{CC}(q)$  remains a smooth function of  $q$ , implying therefore a perfect cancellation of peaks in  $S_{\sigma\sigma'}(q)$ . We also examine  $S_{\sigma\sigma'}(q)$  for an ideal 1V2DES at  $\zeta = 0$ , where QMC simulations<sup>31</sup> are available to check the accuracy of theory. A direct comparison (see Fig. 3) reveals that both  $S_{\sigma\sigma'}(q)$  and  $S_{CC}(q)$  agree nicely with the QMC data for  $r_s < r_s^c$ , but thereafter only  $S_{CC}(q)$  remains close to the simulation results. Particularly, the

sharp peaks in the STLS  $S_{\sigma\sigma'}(q)$  for  $r_s > r_s^c$  are in complete contrast with the QMC study. Thus, as in a 3DES, the STLS theory fails to handle the spin-resolved correlations in 2DES for  $r_s > r_s^c$ , but it provides a fairly good description of the spin-summed correlations. A qualitatively similar picture is found for an ideal 2V2DES and the quasi 1V2DES. For a ready reference,  $r_s^c$  is given in Fig. 4 at selected  $\zeta$  for the quasi- and ideal-2DESs.

### B. Ground-state energy and correlation energy

The Eqs. (10)-(12) can be combined to rewrite the ground-state energy in reduced units as

$$E_0(r_s, \zeta) = \frac{1+\zeta^2}{g_v r_s^2} + \frac{2}{r_s} \sqrt{\frac{1+\zeta}{2g_v}} \int_0^1 d\lambda \int_0^\infty dq F(q) \times [S_{CC}(q; r_s, \lambda) - 1]. \quad (16)$$

It is important to mention here that we have computed the potential energy by performing integration over  $\lambda$  and not over the  $r_s$  parameter. This is rather necessary for the quasi 2DES as the form factor  $F(q)$  here is a function of  $r_s$ . Further, since the calculation of  $E_0$  involves only  $S_{CC}(q)$  and the STLS theory yields a reliable  $S_{CC}(q)$  despite the emergence of unphysical poles in  $\chi_{\sigma\sigma'}(q, \omega)$  for  $r_s$  above  $r_s^c$ , we trust that our results of  $E_0$  should be reliable for  $r_s > r_s^c$  also. We have checked this point explicitly at  $\zeta = 0$  by comparing  $E_0$  computed via  $S_{\sigma\sigma'}(q)$  and through the direct calculation of  $S_{CC}(q)$  which does not involve poles and is possible only at  $\zeta = 0$  and 1. To our satisfaction, the two results matched within the tolerance of self-consistent calculation.

In Fig. 5(a) we report  $E_0(r_s, \zeta)$  for the quasi 2V2DES at selected  $\zeta$  over a wide range of  $r_s$ . Owing to overlapping of different energy curves for  $r_s \gtrsim 7$ , we have

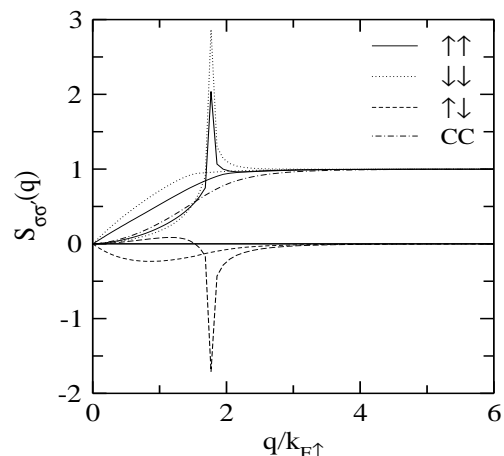


FIG. 1: The spin-resolved static structure factors  $S_{\sigma\sigma'}(q)$  vs  $q/k_{F\uparrow}$  at  $\zeta = 0.25$ , and  $r_s = 2$  and 4 (the curves with sharp peaks) for the quasi 2V2DES. The dashed-dot curve represents the total charge-charge static structure factor  $S_{CC}(q)$  at  $r_s = 4$ .

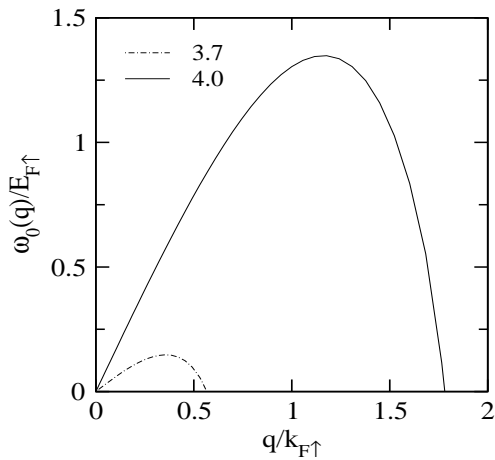


FIG. 2: The pole position  $\omega_0(q)$  vs  $q/k_{F\uparrow}$  at  $\zeta = 0.25$  for the quasi 2V2DES. Legends indicate the value of  $r_s$  and  $E_{F\uparrow}$  is the Fermi energy of the  $\uparrow$  spin electrons.

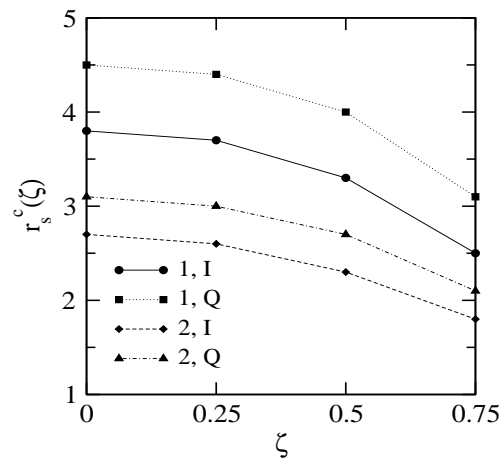


FIG. 4: Critical  $r_s$  (i.e.,  $r_s^c$ ) for the onset of pole in  $\chi_{\sigma\sigma'}(q, \omega)$  vs  $\zeta$ ; in each case the first legend stands for the value of  $g_v$ , while the second for the quasi (Q) or ideal (I) 2DES models. Lines are just a guide to the eye.

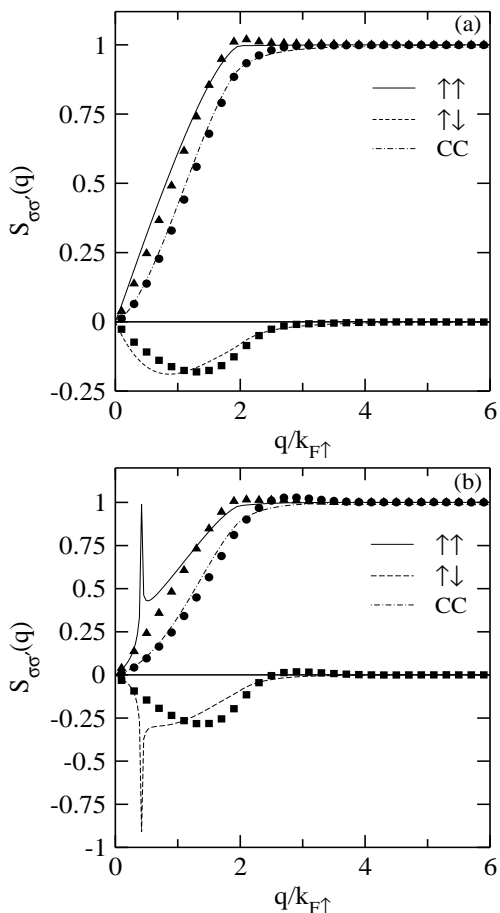


FIG. 3: The spin-resolved ( $S_{\sigma\sigma'}(q)$ ) and the total charge-charge ( $S_{CC}(q)$ ) structure factors vs  $q/k_{F\uparrow}$  at  $\zeta = 0$ , and  $r_s = 2$  [in panel (a)] and  $5$  [in panel (b)] for an ideal 1V2DES. The symbols are the QMC data taken from the Ref. 31.

depicted in Fig. 5(b) the energy difference  $\{E_0(r_s, \zeta) - E_0(r_s, 0)\}$  at different  $\zeta$  to resolve the stable spin phase.

One may note that the unpolarized ( $\zeta = 0$ ) phase remains stable up to  $r_s \approx 13.2$  and then, there occurs an abrupt transition to the polarized ( $\zeta = 1$ ) phase, with the partially spin-polarized states remaining unstable. A qualitatively similar result is found to hold for the quasi 1V2DES (see Fig. 6), where the spin-polarization transition takes place at  $r_s \approx 8$ . However, in order to get a clear picture of the ground state, we must analyze the 1V and 2V cases together. Accordingly, we plot in Fig. 6 the energy difference  $\{E_{0,g_v}(r_s, \zeta) - E_{0,2}(r_s, 0)\}$  for  $g_v = 2$  and  $1$  at different  $\zeta$ . It may be pointed out that  $E_0$  for the polarized 2V state is equal to that for the unpolarized 1V state. Apparently, the unpolarized 2V phase represents the ground state for  $r_s < 8.8$ , and there occurs at  $r_s \approx 8.8$  a first-order transition to the polarized 1V phase (i.e., simultaneous valley- and spin-polarization) before there could happen a transition to the polarized 2V phase. Thus, we find that the partially spin-polarized phases are unstable in the Si (100) inversion layer. Moreover, our prediction of the unpolarized 2V ground state for  $r_s < 8.8$  is in agreement with the experiment of Pudalov *et al.*<sup>9</sup>, where the electron states have been observed to be four-fold degenerate over the investigated density range of  $1.5 < r_s < 8.4$ .

For assessing the role of the finite width of 2DES, we report in Fig. 7  $E_0(r_s, \zeta)$  for the ideal 2DES. Qualitatively, a phase diagram similar to the quasi 2DES is obtained, with the simultaneous valley- and spin-polarization now occurring at  $r_s \sim 6.7$ . In agreement with the QMC study<sup>4,13</sup>, the partially spin-polarized states are unstable irrespective of the valley degeneracy. Analyzing separately the 1V and 2V results, we notice however that both support a first-order spin-polarization transition at a sufficiently low  $r_s$ . In the 1V2DES this transition agrees qualitatively with the QMC study<sup>4</sup>, though the  $r_s$  for the transition is underestimated by about a factor of 4; however its occurrence in the 2V2DES grossly disagrees

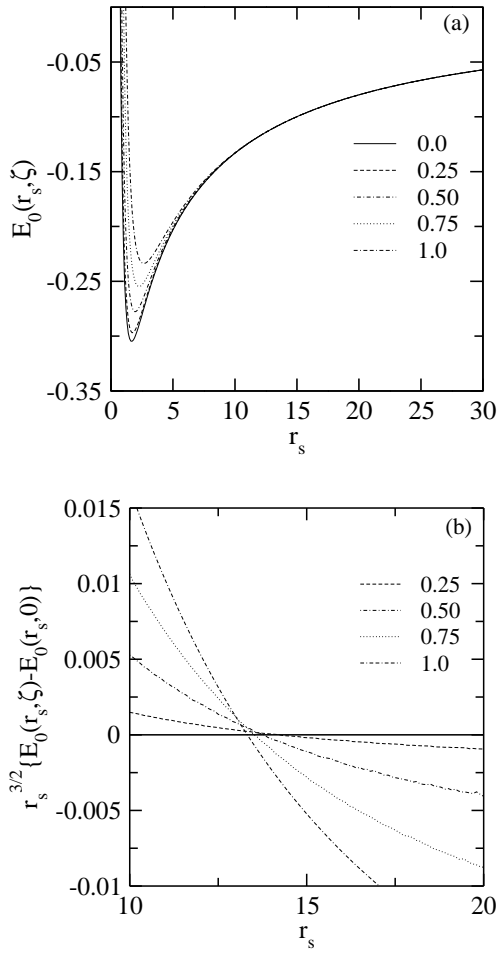


FIG. 5: The ground-state energy  $E_0(r_s, \zeta)$  [in panel (a)] and  $r_s^{3/2}\{E_0(r_s, \zeta) - E_0(r_s, 0)\}$  [in panel (b)] plotted as a function of  $r_s$  at different  $\zeta$  for the quasi 2V2DES; legends indicate the value of  $\zeta$ .

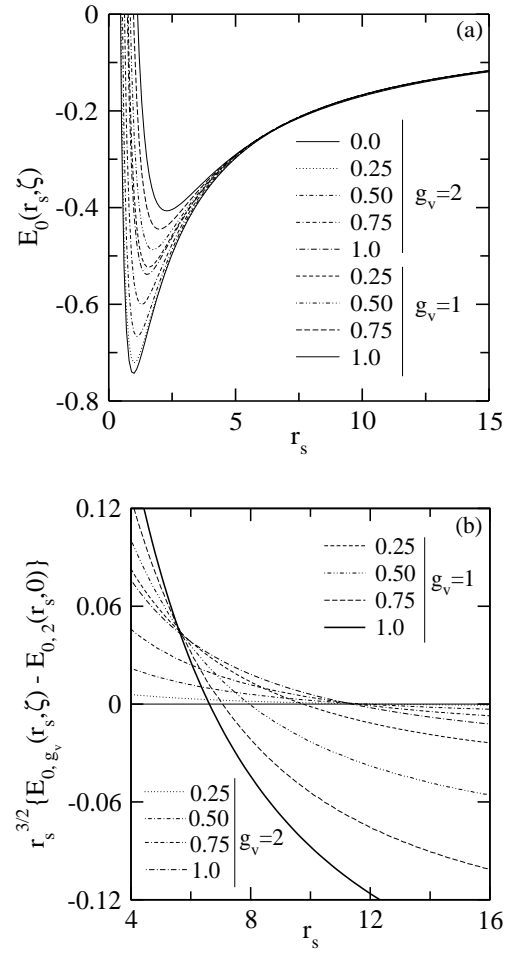


FIG. 7: The curves are labeled in the same manner as in Fig. 6 except that the results are for the ideal 2DES.

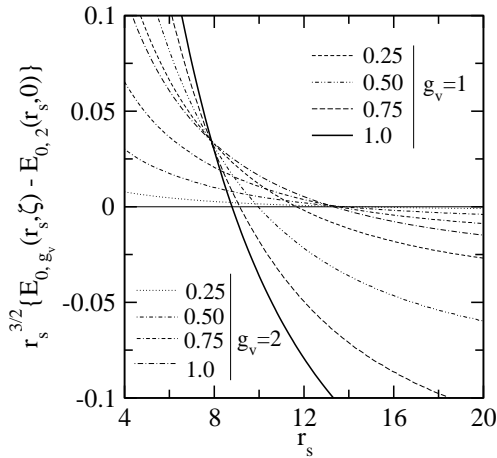


FIG. 6:  $r_s^{3/2}\{E_{0, g_v}(r_s, \zeta) - E_{0, 2}(r_s, 0)\}$  plotted as a function of  $r_s$  at different  $\zeta$  by taking  $g_v = 2$  and 1 for the quasi 2DES; legends indicate the value of  $\zeta$ .

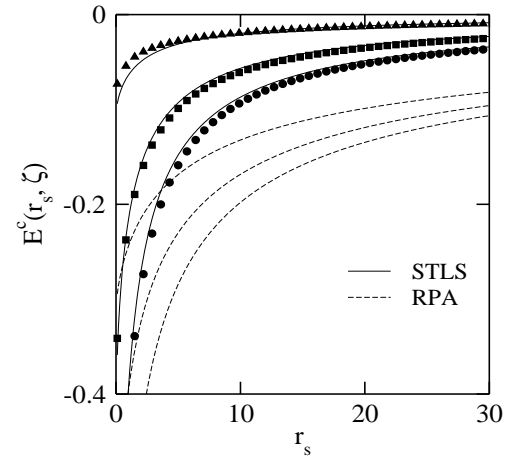


FIG. 8: The correlation energy  $E^c(r_s, \zeta)$  vs  $r_s$  for an ideal 2V- and 1V-2DES (from bottom to top) at  $\zeta = 0$  and 1 within the STLS and RPA approximations. The symbols represent the QMC data taken from the Refs. 4 (1V) and 13 (2V).

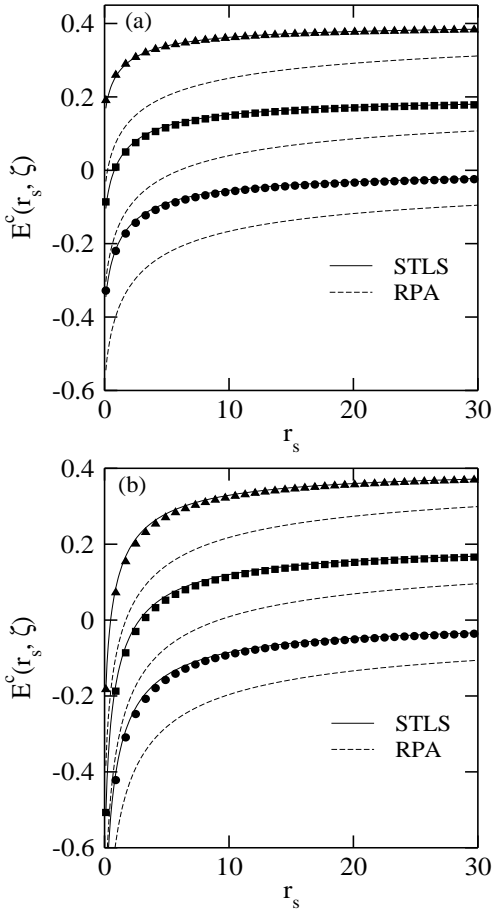


FIG. 9: The correlation energy  $E^c(r_s, \zeta)$  vs  $r_s$  for an ideal 2DES at  $\zeta=0.25, 0.50$ , and  $0.75$  (from bottom to top) within the STLS and RPA approximations for 1V [in panel (a)] and 2V [in panel (b)]. The symbols represent the QMC data taken from the Refs. 4 (1V) and Ref. 13 (2V). For clarity,  $E^c(r_s, \zeta)$  at  $\zeta=0.50$  and  $0.75$  has been shifted vertically by  $0.2$  and  $0.4$ , respectively.

with the QMC simulations<sup>13,32</sup> where the unpolarized 2V phase has been found to represent the ground state for densities down to the Wigner crystallization. To understand this qualitative mismatch, we compare in Figs. 8 and 9 the STLS correlation energy  $E^c(r_s, \zeta)$  with the QMC data<sup>4,13</sup> at different  $\zeta$  and  $g_v$ . The RPA results are also shown to demonstrate the importance of short-range correlations. Evidently, the STLS results are in very good agreement with the QMC study both for  $g_v = 1$  and  $2$ , and the RPA badly overestimates the correlation energy. Thus, the situation remains unclear from this comparison.

To get further clue, we analyze in Fig. 10 the fractional difference between the QMC and STLS ground-state energy  $\Delta E_0 = \{E_0^{QMC}(r_s, \zeta) - E_0^{STLS}(r_s, \zeta)\} / E_0^{QMC}(r_s, \zeta)$  for the 1V and 2V systems at  $\zeta = 0$  and  $1$ . Interestingly, the STLS theory underestimates the magnitude of  $E_0$  for the unpolarized 1V and 2V states (with its extent increasing with  $r_s$  and  $g_v$ ), while for the polarized 1V state it

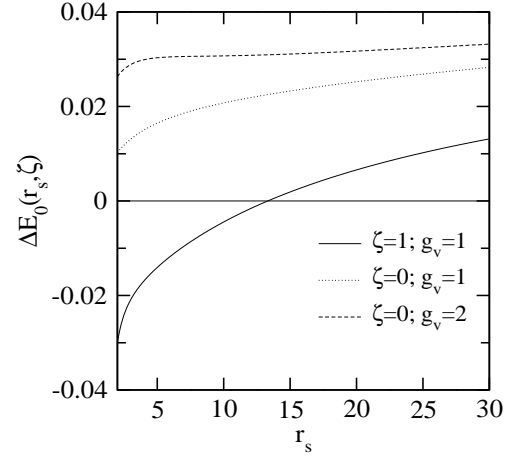


FIG. 10: Fractional energy difference  $\Delta E_0$  between the QMC and STLS results of ground-state energy [i.e.,  $\{E_0^{QMC}(r_s, \zeta) - E_0^{STLS}(r_s, \zeta)\} / E_0^{QMC}(r_s, \zeta)$ ] vs  $r_s$  at indicated  $\zeta$  and  $g_v$ . The QMC data is taken from the Refs. 33 (1V) and 32 (2V).

exhibits overestimation in the  $r_s$ -region where the STLS predicts the valley- and/or spin-polarization transitions. Apparently, it is the opposite sign of  $\Delta E_0$  for the unpolarized 2V and the polarized 1V states which leads to simultaneous valley- and spin-polarization at  $r_s \approx 6.7$ . On the other hand, the spin-polarization in the 2V2DES seems to arise due to a decrease in  $\Delta E_0$  in going from  $\zeta = 0$  to  $1$ .

### C. Spin-resolved interaction energy of correlation

In order to test further the STLS  $S_{\sigma\sigma'}(q)$ , we compute and compare with the available QMC data (as fitted analytically by Gori-Giorgi *et al.*<sup>31</sup>) the correlation contribution to the spin-resolved interaction energy  $v_{\sigma\sigma'}^c(r_s, \zeta)$ , for an ideal 1V2DES. By definition

$$v_{\sigma\sigma'}^c(r_s, \zeta) = E_{\sigma\sigma'}^{int}(\lambda = e^2; r_s, \zeta) - E_{\sigma\sigma'}^x(r_s, \zeta), \quad (17)$$

with

$$E_{\sigma\sigma'}^x(r_s, \zeta) = -\delta_{\sigma\sigma'} \frac{4\sqrt{2}}{3\pi r_s} [1 + (-1)^{\delta_{\sigma\downarrow}} \zeta]^{3/2}, \quad (18)$$

being the exchange contribution to the interaction energy.  $v_{\sigma\sigma'}^c(r_s, \zeta)$  are plotted in Fig. 11 as a function of  $r_s$  at different  $\zeta$ . Results are shown for  $r_s$  up to  $r_s^c$ , because thereafter  $S_{\sigma\sigma'}(q)$  are not reliable due to unphysical poles in  $\chi_{\sigma\sigma'}(q, i\omega)$ . Notably, the STLS theory underestimates the  $\uparrow\uparrow$  and  $\downarrow\downarrow$  contributions, while the  $\uparrow\downarrow$  part is overestimated to an extent that the spin summed result (i.e.,  $v_{\uparrow\uparrow}^c + v_{\downarrow\downarrow}^c + v_{\uparrow\downarrow}^c$ ) lies close to the QMC data. The degree of underestimate is more for the  $\downarrow\downarrow$  (i.e., the dilute spin) component, with its value becoming small positive against the QMC result beyond a certain  $r_s$ . The cross-spin correlation dominates over the like-spin

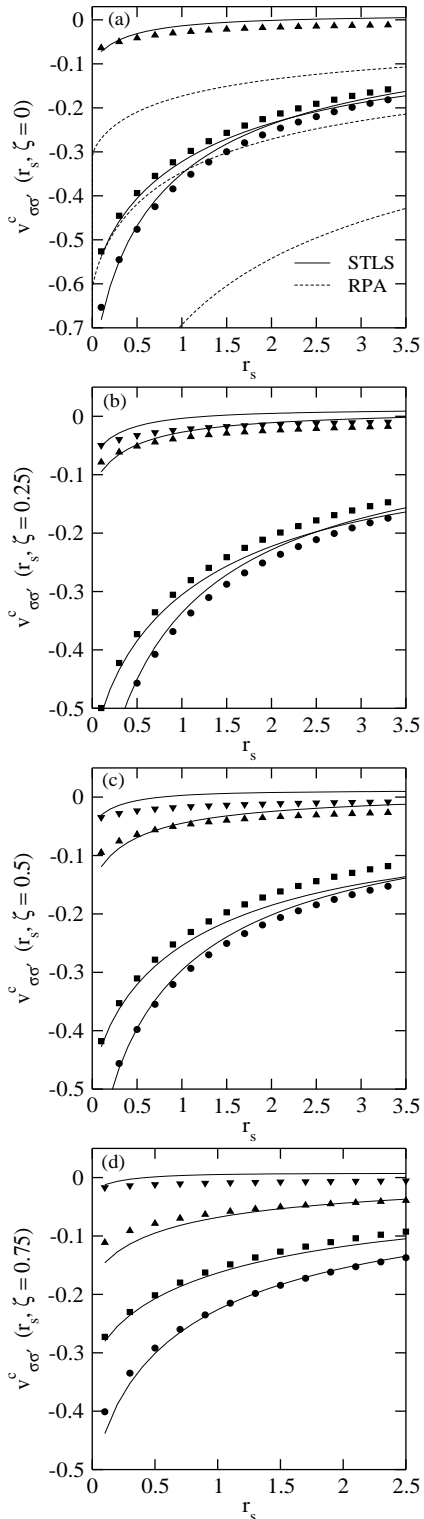


FIG. 11: The spin-resolved interaction energy of correlation  $v_{\sigma\sigma'}^c(r_s, \zeta)$  vs  $r_s$  at selected  $\zeta$  for an ideal 1V2DES. The symbols are the QMC data as fitted by Gori-Giorgi *et al.*<sup>31</sup> In each case, the curves and symbols from top to bottom represent, respectively, the  $\downarrow\downarrow$ ,  $\uparrow\uparrow$ ,  $\uparrow\downarrow$ , and the spin summed (i.e.,  $v_{\uparrow\uparrow}^c + v_{\downarrow\downarrow}^c + v_{\uparrow\downarrow}^c$ ) contributions.

contribution meaning thereby the latter are determined mainly by the exchange effects. Furthermore, a comparison with the RPA reveals that it overestimates all three correlation components, with the like-spin part showing the maximum departure from the QMC data; this point is illustrated in Fig. 11(a) at  $\zeta = 0$ .

#### D. Spin susceptibility

The spin susceptibility  $\chi_s$  is computed (from Eq. (13)) for three different devices, viz. the Si (100) inversion layer, the AlAs QW, and the GaAs HIGFET. For the AlAs QW, we employ the infinite QW model where<sup>34</sup>

$$F(q) = \frac{1}{4\pi^2 + q^2 a^2} \left( 3qa + \frac{8\pi^2}{qa} - \frac{32\pi^4}{q^2 a^2} \frac{1 - e^{-qa}}{4\pi^2 + q^2 a^2} \right), \quad (19)$$

with  $a = 4.5\text{nm}$  being the width of the well. In case of the GaAs HIGFET,  $F(q)$  can be obtained<sup>35</sup> from Eq. (2) by setting  $\epsilon_{ins} = \epsilon_{sc}$  and taking  $\epsilon = 12.9$ ,  $m_z = 0.067m_e$ , and  $n_d = 0$ <sup>15</sup>.

Figure 12 depicts our  $\chi_s/\chi_P$  for the Si (100) inversion layer, along with the experimental data of Pudalov *et al.*<sup>22</sup> and Shashkin *et al.*<sup>7</sup>, and the QMC and STLS results for an ideal 2V2DES model. To see the effect of valley degeneracy, the STLS and QMC results<sup>4</sup> are also given at  $g_v = 1$ . However, we should look for a comparison at  $g_v = 2$  as the 2V unpolarized phase is found to represent the ground state over the  $r_s$  range where experimental  $\chi_s$  is available. It is gratifying to note that  $\chi_s$  for  $g_v = 2$  exhibits very good agreement with the experiment, except at the largest  $r_s$  values, near the apparent ferromagnetic instability found in Ref. 7. Importantly,

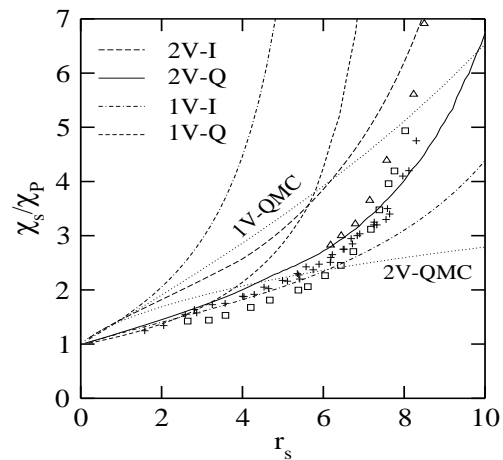


FIG. 12: The spin susceptibility enhancement  $\chi_s/\chi_P$  vs  $r_s$  for the quasi (Q) and ideal (I) models of the Si (100) inversion layer. The symbols represent the experimental data of Pudalov *et al.*<sup>22</sup> and Shashkin *et al.*<sup>7</sup> The dotted curves represent, respectively, the QMC results for the ideal 1V (Ref. 4) and 2V (Ref. 13) 2DESs. The dashed-dot curve is the RPA result for the quasi Si (100) inversion layer.



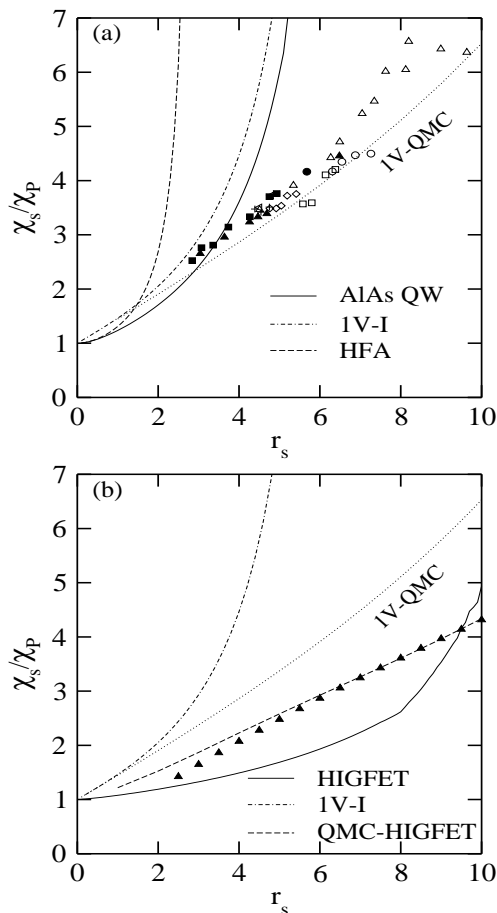


FIG. 13: The spin susceptibility enhancement  $\chi_s/\chi_P$  vs  $r_s$  for the AlAs QW [in panel (a)] and the GaAs HIGFET [in panel (b)], along with the STLS (double dashed-dot lines) and QMC<sup>4</sup> (dotted lines) results for an ideal (I) 1V2DES. The symbols represent the respective experimental results of Vakili *et al.*<sup>10</sup> and Zhu *et al.*<sup>11</sup> In (a) dashed curve is the HFA result for an ideal 1V2DES, while in (b) it refers to the thickness corrected QMC result for the GaAs HIGFET due to Depalo *et al.*<sup>15</sup>

it is crucial to include in the theory both the valley degeneracy and the finite thickness of the 2DES. Both of these factors act to suppress  $\chi_s/\chi_P$  appreciably over the ideal 1V2DES estimate. Indeed, considering the sizeable disagreement between STLS and QMC predictions for the strictly 2D systems, the good agreement found with the experiment up to  $r_s \approx 7.5$  can only be understood in terms of the dominance of thickness over correlation effects<sup>15</sup>. Similar results have been reported recently by De Palo *et al.*<sup>15</sup> and Zhang and Das Sarma<sup>16</sup>.

Although not reported here, it is consistent to find that  $\chi_s$  tends to diverge near the spin-polarization transition. For the Si (100) system, the divergence occurs at  $r_s \sim 13$ , which lies close to the experimental estimate<sup>36</sup> of the critical  $r_s$  for the ferromagnetic instability.

Next we show in Fig. 13  $\chi_s/\chi_P$  for the AlAs QW and the GaAs HIGFET, together with the respective ex-

perimental data<sup>10,11</sup> and the STLS results for the ideal 1V2DES. Once again we note that the inclusion of the finite width of the 2DES brings the STLS predictions closer to the experiment. However, the AlAs QW being much narrower exhibits comparatively smaller suppression due to finite thickness and the agreement is much less satisfactory than for the Si (100) system, both for the AlAs QW and the GaAs HIGFET.

Interestingly, the quality of the STLS predictions is different in three systems. This seems to suggest that it might be important to include other device specific parameters like disorder<sup>37</sup>. Moreover, the choice of confining potential is expected to affect the form factor and hence, the interaction potential; for instance, taking a finite (AlAs) QW model would result in a softer potential and therefore, in suppression of  $\chi_s$  over the infinite QW result. Likewise, in the inversion layer model Stern and Howard<sup>23</sup> did not consider the exchange-correlation effects in calculating the interface electronic eigenfunctions. Later on Ando<sup>38</sup> found that these effects reduce the width of inversion layer, which in turn is expected to enhance  $\chi_s$ .

#### IV. SUMMARY AND CONCLUSIONS

To summarize, we have investigated the spin properties of a 2DES, as realized at the interface of semiconductor-insulator/semiconductor heterojunctions, by using the STLS approach. The Si (100) inversion layer has been studied in detail to calculate the spin-resolved static structure factors and the ground-state energy at arbitrary  $\zeta$  over a wide range of  $r_s$ . We deduce quite generally that the STLS theory fails in determining the spin-resolved correlations above a critical  $r_s$  due to the appearance of unphysical poles in  $\chi_{\sigma\sigma'}(q, \omega)$ , i.e., at imaginary frequency. Such poles, however, may be shown to not contribute to the frequency integral of  $\chi''_{\sigma\sigma'}(q, \omega)$  yielding the structure factors, which can still be computed, and the spin summed properties (such as the charge-charge structure factor) remain reliable and close to the available QMC simulation data.

This enabled us to determine the ground-state energy over a wide range of  $r_s$  at arbitrary  $\zeta$  and hence, the stable spin phase. For the quasi Si (100) system, the unpolarized 2V phase is found to represent the ground state for  $r_s \lesssim 8.8$  and thereafter, a first-order transition occurs to the polarized 1V phase. The predicted ground state for  $r_s \lesssim 8.8$  agrees with the experiment of Pudalov *et al.*<sup>9</sup> Furthermore, the calculated spin susceptibility agrees fairly well with the experiment, but only with the inclusion of transverse thickness and valley degeneracy, provided one does not come too close to the apparent ferromagnetic instability found in Ref. 7.

Without thickness we find that STLS sizeably overestimates the spin susceptibility, both for the 1V and 2V states, a drawback in common with RPA<sup>13,15</sup>. The spin susceptibility has also been calculated for the 2DESs as

realized in the AlAs QW and the GaAs HIGFET. We find that agreement with experiment is much less satisfactory in these cases, even though it is somewhat improved by the inclusion of thickness.

For the ideal (i.e., zero thickness) 2DES model, the STLS theory reproduces nicely the recent QMC correlation energy at arbitrary  $\zeta$  both for the 1V and 2V states. However, the agreement is seen to depend qualitatively on  $\zeta$  and  $g_v$ . Particularly, the correlation energy is overestimated for the 1V state at  $\zeta = 1$ , whereas it is underestimated for the 2V state both at  $\zeta = 0$  and at  $\zeta = 1$ . Although the magnitude of deviation from the QMC data is small, yet this being of opposite sign causes simultaneous valley- and spin-polarization at  $r_s \sim 6.7$ , a prediction

in gross violation of the QMC study. An analysis of the correlation contribution to the spin-resolved interaction energy reveals that the STLS theory is relatively less accurate in handling the like-spin correlations. This result may have bearing on the further development of the theory of electron correlation.

## ACKNOWLEDGEMENTS

The authors are grateful to Paola Gori-Giorgi for providing the QMC simulation data of spin-resolved pair-correlation functions.

- 
- \* rkmoudgil@kuk.ac.in
- <sup>1</sup> T. Ando, A. B. Fowler, and F. Stern, *Rev. Mod. Phys.* **54**, 437 (1982); A. Isihara, *Solid State Phys.* **42**, 271 (1989).
  - <sup>2</sup> See, for instance, D. D. Awschalom, N. Samarth, and D. Loss, *Semiconductor Spintronics and Quantum Computing*, (Springer-Verlag, Berlin, 2002).
  - <sup>3</sup> G. Senatore, S. Moroni, and D. Varsano, *Solid State Commun.* **119**, 333 (2001); D. Varsano, S. Moroni, and G. Senatore, *Europhys. Lett.* **53**, 348 (2001).
  - <sup>4</sup> C. Attacalite, S. Moroni, P. Gori-Giorgi, and G. B. Bachelet, *Phys. Rev. Lett.* **88**, 256601 (2002).
  - <sup>5</sup> G. Ortiz, M. Harris, and P. Ballone, *Phys. Rev. Lett.* **82**, 5317 (1999); F. H. Zong, C. Lin, and D. M. Ceperley, *Phys. Rev. E* **66**, 036703 (2002).
  - <sup>6</sup> A. A. Shashkin, S. V. Kravchenko, V. T. Dolgoplov, and T. M. Klapwijk, *Phys. Rev. Lett.* **87**, 086801 (2001).
  - <sup>7</sup> A. A. Shashkin, S. Anissimova, M. R. Sakr, S. V. Kravchenko, V. T. Dolgoplov, and T. M. Klapwijk, *Phys. Rev. Lett.* **96**, 036403 (2006), and references therein.
  - <sup>8</sup> S. A. Vitkalov, H. Zheng, K. M. Mertez, M. P. Sarachik, and T. M. Klapwijk, *Phys. Rev. Lett.* **87**, 086401 (2001).
  - <sup>9</sup> V. M. Pudalov, M. E. Gershenson, and H. Kojima, *cond-mat/0110160V1* (2001).
  - <sup>10</sup> K. Vakili, Y. P. Shkolnikov, E. Tutuc, E. P. De Poortere, and M. Shayegan, *Phys. Rev. Lett.* **92**, 226401 (2004).
  - <sup>11</sup> J. Zhu, H. L. Stormer, L. N. Pfeiffer, K. W. Baldwin, and K. W. West, *Phys. Rev. Lett.* **90**, 056805 (2003).
  - <sup>12</sup> Y. P. Shkolnikov, K. Vakili, E. P. De Poortere, and M. Shayegan, *Phys. Rev. Lett.* **92**, 246804 (2004).
  - <sup>13</sup> M. Marchi, S. De Palo, S. Moroni, and Gaetano Senatore, *Phys. Rev. B* **80**, 035103 (2009).
  - <sup>14</sup> S. Yarlagadda and G. F. Giuliani, *Phys. Rev. B* **38**, 10966 (1988); *ibid* **40**, 5432 (1989).
  - <sup>15</sup> S. De Palo, M. Botti, S. Moroni, and Gaetano Senatore, *Phys. Rev. Lett.* **94**, 226405 (2005); *ibid* **97**, 039702 (2006).
  - <sup>16</sup> Ying Zhang and S. Das Sarma, *Phys. Rev. B* **72**, 075308 (2005); 115317 (2005).
  - <sup>17</sup> A. K. Rajagopal, S. P. Singhal, M. Banerjee, and J. C. Kimball, *Phys. Rev. B* **17**, 2262 (1978).
  - <sup>18</sup> B. Davoudi and M. P. Tosi, *Physica B: Condensed Matter*, **322**, 124 (2002).
  - <sup>19</sup> K. S. Singwi, M. P. Tosi, R. H. Land, and A. Sjölander, *Phys. Rev.* **176**, 589 (1968).
  - <sup>20</sup> M. Jonson, *J. Phys. C* **9**, 3055 (1976).
  - <sup>21</sup> A. Gold, *Phys. Rev. B* **50**, 4297 (1994).
  - <sup>22</sup> V. M. Pudalov, M. E. Gershenson, H. Kojima, N. Butch, E. M. Dizhur, G. Brunthaler, A. Prinz, and G. Bauer, *Phys. Rev. Lett.* **88**, 196404 (2002).
  - <sup>23</sup> F. Stern and W. E. Howard, *Phys. Rev.* **163**, 816 (1967).
  - <sup>24</sup> W. J. Bloss, L. J. Sham, and B. Vinter, *Phys. Rev. Lett.* **43**, 1529 (1979); A. Isihara and L. C. Ioriatti, Jr., *Phys. Rev. B* **25**, 5534 (1982).
  - <sup>25</sup> A. Sjölander and M. J. Stott, *Phys. Rev. B* **5**, 2109 (1971).
  - <sup>26</sup> See, for instance, G. D. Mahan, *Many-Particle Physics*, 2nd ed. (Plenum, New York, 1990).
  - <sup>27</sup> See for example, L. D. Landau and E. M. Lifshitz, *Statistical Physics*, 3rd ed. part 1 (Pergamon Press, 1980).
  - <sup>28</sup> R. K. Moudgil, P. K. Ahluwalia, and K. N. Pathak, *Phys. Rev. B* **51**, 1575 (1995).
  - <sup>29</sup> Krishan Kumar, Vinayak Garg, and R. K. Moudgil, *Phys. Rev. B* **79**, 115304 (2009).
  - <sup>30</sup> Vinayak Garg, R. K. Moudgil, Krishan Kumar, and P. K. Ahluwalia, *Phys. Rev. B* **78**, 045406 (2008).
  - <sup>31</sup> Paola Gori-Giorgi, Saverio Moroni, and Giovanni B. Bachelet, *Phys. Rev. B* **70**, 115102 (2004).
  - <sup>32</sup> S. Conti and G. Senatore, *Europhys. Lett.* **36**, 695 (1996).
  - <sup>33</sup> F. Rapisarda and G. Senatore, *Aust. J. Phys.* **49**, 161 (1996).
  - <sup>34</sup> A. Gold, *Phys. Rev. B* **35**, 723 (1987).
  - <sup>35</sup> F. C. Zhang and S. Das Sarma, *Phys. Rev. B* **33**, 2903R (1986), and references therein.
  - <sup>36</sup> V. M. Pudalov, M. E. Gershenson, and H. Kojima, *cond-mat/0110160V2* (2002).
  - <sup>37</sup> G. Fleury and X. Waintal, *Phys. Rev. B* **81**, 165117 (2010).
  - <sup>38</sup> A. Ando, *Phys. Rev. B* **13**, 3468 (1975).